ROBUST YAW STABILITY CONTROL FOR ELECTRIC VEHICLES BASED ON ACTIVE FRONT STEERING CONTROL THROUGH A STEER-BY-WIRE SYSTEM

K. NAM[1)*], S. OH[1)], H. FUJIMOTO[2)] and Y. HORI[2)]

[1)]Department of Electrical Engineering, The University of Tokyo, Tokyo 113-0033, Japan
[2)]Department of Advanced Energy, The University of Tokyo, Chiba 277-856, Japan

ABSTRACT–A robust yaw stability control design based on active front steering control is proposed for in-wheel-motored electric vehicles with a Steer-by-Wire (SbW) system. The proposed control system consists of an inner-loop controller (referred to in this paper as the steering angle-disturbance observer (SA-DOB), which rejects an input steering disturbance by feeding a compensation steering angle) and an outer-loop tracking controller (i.e., a PI-type tracking controller) to achieve control performance and stability. Because the model uncertainties, which include unmodeled high frequency dynamics and parameter variations, occur in a wide range of driving situations, a robust control design method is applied to the control system to simultaneously guarantee robust stability and robust performance of the control system. The proposed control algorithm was implemented in a CaSim model, which was designed to describe actual in-wheel-motored electric vehicles. The control performances of the proposed yaw stability control system are verified through computer simulations and experimental results using an experimental electric vehicle.

1. INTRODUCTION

Due to drastically increasing concerns in eco-friendly vehicles and the electrification of vehicle systems, there has been a great deal of research on electric vehicles. In contrast to conventional internal combustion engine vehicles, in-wheel-motored electric vehicles are directly driven by electric motors that are installed in each wheel. From an energy perspective, this means that the complicated power transfer apparatus, which includes a clutch, transmission, and gear box, is not required, which contributes to increasing the energy efficiency. Moreover, electric vehicles can provide emission-free urban transportation (Chan, 2002). Regarding vehicle dynamics control, electric vehicles also have attractive advantages over internal combustion engine vehicles. Three remarkable advantages of electric vehicles have been summarized (Hori, 2004; Sakai *et al.*, 1999):

- The torque generation of driving motors is very fast and accurate, which can enhance control performance regarding wheel-slip and yaw stability.
- The driving torque can be easily measured from the

motor current, which enables the estimation of the driving forces of each wheel and the road conditions.
- It is possible to independently control each wheel's torque based on in-wheel motors installed in each wheel.

There are two available methods to enhance vehicle yaw stability for in-wheel-motored electric vehicles: a direct yaw moment control method using independent in-wheel motor control and an active front steering control method (Falcone and Murakami, 2007; Ohara *et al.*, 2008). The direct yaw moment control method for electric vehicles based on independent driving torque control was proposed and evaluated through experiments (Fujimoto *et al.*, 2004, 2005). Robust yaw stability control based on active steering control for road vehicles was designed, and its performance was verified through a Hardware-in-the-Loop simulation (Guvenc *et al.*, 2009). A disturbance observer (DOB) design method, based on mapping frequency domain performance criteria to model the regulator parameter space, was introduced (Guvenc *et al.*, 2004, 2009). Two different robust feedback controllers, which are based on internal model control and sliding mode control approaches, were designed, and their control performances were verified through extensive simulation tests (Canale *et al.*, 2009).

In this paper, a second approach (i.e., yaw stability

Corresponding author. e-mail: nkh6189@gmail.com

control by active front steering control) was applied (Nam et al., 2010), and the application of an SbW system to electric vehicles was evaluated through simulation and experimental results. The actual implementation of the active front steering controller will be much easier when the SbW system becomes commercially available. In the SbW system, the driver's steering wheel is no longer mechanically connected to the steering tires. The driver's steering command is electrically transmitted to the electric power steering (EPS) motor, which moves the tires directly. With SbW systems, there is a great potential for enhanced safety of the occupants in a vehicle due to the fast and precise intervention that is in contrast to the limited reaction time of the driver (e.g., the maximum reaction time of a driver is approximately 0.5 sec) (Ackermann and Bünte, 1997). Therefore, accurate steering control based on the fast intervention of SbW systems can provide enhanced safety and handling performance relative to the steering action of a skilled driver. This motivates active steering control based on feedback control. In addition, human-friendly steering control through driver-SbW interaction is required to simultaneously provide improved safety and steering feeling, which may potentially be problematic in practical applications to commercial vehicles.

There are two different possibilities for using the front steering angle as a control input. The first possibility is to add, in the electronic control unit, the steering controller output (auxiliary steering angle) to the steering signal that comes from the driver. In this case, the total front steering angle is set by an SbW actuator. In this study, the second possibility, in which the auxiliary steering angle is added mechanically, is applied. Therefore, an auxiliary steering actuator is required, and consequently, the range of the auxiliary steering angle will be limited. This causes the risk of actuator saturation in the presence of model errors or disturbances (Guvenc et al., 2004). It is noted that in this study, the motion of the auxiliary steering actuator is transmitted to the tire but not to the driver's steering wheel. Thus, there is no problem associated with the driver perceiving additional steering action in the steering wheel because of the steering controller.

The aim of this paper is to present a robust control strategy for the active front steering system to protect the vehicle from spin-out and drift-out and to realize improved cornering performance by controlling yaw motion. Robust control methodology, which is a two-degrees-of-freedom control based on the disturbance observer, is used to enhance the robustness against model uncertainties and external disturbances. In the controller design, a robust control design method (Doyle et al., 1992) is used to achieve robust control performances and satisfy the stability conditions. A proposed controller has two control loops: 1) The Q-filter (Umeno and Hori, 1991) in an inner loop steering angle-disturbance observer (SA-DOB) is designed to reject disturbances in the low frequency region. 2) The outer loop tracking controller (i.e., the two-degrees-of-
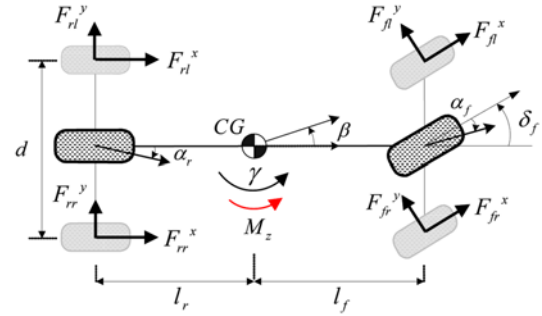

Figure 1. Three-DOF yaw plane vehicle model.

freedom controller) is designed to enhance yaw rate tracking performance. Computer simulations and field tests were conducted to evaluate the control performance of the proposed control system. The simulation and experimental results show that the proposed yaw stability controller is effective at rejecting disturbances and improving yaw tracking performance.

2. VEHICLE MODELING

A commonly used planar vehicle model is introduced to account for longitudinal and lateral behaviors and the yaw motion as shown in Figure 1.

The governing equations for longitudinal and lateral motions are given by

$$ma_x = \sum_{i=1}^{2}(F_i^x\cos\delta_f - F_i^y\sin\delta_f) + \sum_{i=3}^{4}F_i^x \qquad (1)$$

$$ma_y = \sum_{i=1}^{2}(F_i^x\sin\delta_f + F_i^y\cos\delta_f) + \sum_{i=3}^{4}F_i^y \qquad (2)$$

where m is the vehicle mass; a_x and a_y are the longitudinal and lateral vehicle accelerations, respectively; F_i^x and F_i^y are the longitudinal and lateral tire forces of the ith tire (i=1,2,3,4 corresponding to fl, fr, rl, rr), respectively; and δ_f is the front steering angle.

The yaw moment balance equation with respect to the center of gravity (CG) is expressed as

$$I_z\dot{\gamma} = \sum_{i=1}^{2}l_f(F_i^x\sin\delta_f + F_i^y\cos\delta_f) - \sum_{3}^{}l_rF_i^y + M_z \qquad (3)$$

where I_z is the yaw moment of inertia; γ is the yaw rate; l_f and l_r are the distance from CG to the front and rear axles, respectively; and M_z indicates a direct yaw moment control input, which is generated by the independent torque control of the in-wheel motors.

For control design simplicity, the linearized single track vehicle model (called a bicycle model) is generally used, and in this paper, it was utilized in controller design. Complex and nonlinear lateral tire forces can be linearized
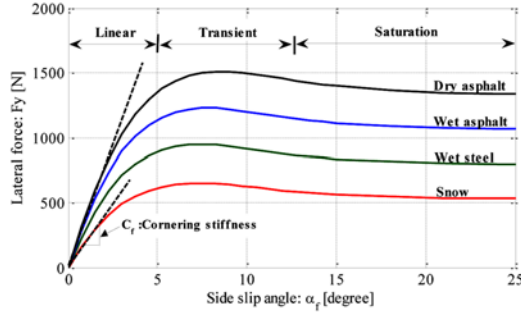
Figure 2. Characteristic curves of lateral tire force.

at linear tire regions (i.e., small tire slip angle regions) and are expressed as follows:

$$F_f^y = -2C_f\alpha_f = -2C_f\left(\beta + \frac{\gamma l_f}{v_x} - \delta_f\right) \tag{4}$$

$$F_r^y = -2C_r\alpha_r = -2C_r\left(\beta - \frac{\gamma l_r}{v_x}\right) \tag{5}$$

where C_f and C_r are the tire cornering stiffness of front and rear tires, respectively; α_f and α_r are the tire side slip angles; β is the vehicle side slip angle; and F_f^y and F_r^y are the lateral tire forces of front and rear tires, respectively.

Figure 2 shows the characteristic curves of the lateral tire force with respect to tire side slip. In regions of small tire slip angle (e.g., up to 5 degrees), the lateral tire forces increase linearly with respect to the increase in the slip angle and can be controlled for yaw stability enhancement by controlling the front steering angle.

From linearized yaw dynamics and tire models, a nominal vehicle yaw model can be obtained as follows:

$$\begin{aligned} I_z\dot{\gamma} &= l_f F_f^y - l_r F_r^y + M_d \\ &= 2l_f C_f \delta_f - \frac{2\gamma(l_f^2 C_f + l_r^2 C_r)}{v_x} + \tilde{M}_d \end{aligned} \tag{6}$$

where M_d represents the unexpected yaw moment disturbances caused by unstable road conditions (e.g., split-μ road), unbalanced tire pressures, and external forces (e.g., side wind), M_d is defined as a lumped yaw moment disturbance and expressed as

$$\tilde{M}_d = -2\beta(l_f C_f - l_r C_r) + M_d \tag{7}$$

From (6) and (7), a transfer function for the nominal vehicle yaw model is obtained as

$$P_n(s) = \frac{2C_f l_f}{I_z s + \left(\frac{l_f^2 C_f + l_r^2 C_r}{v_x}\right)} \tag{8}$$

Here, C_f and C_r are the nominal tire cornering stiffness parameters, which are the values for dry asphalt conditions (i.e., μ = 0.9)

Table 1. Specifications of the experimental electric vehicle.

Parameter	Value
Weight	875 kg
Yaw moment of inertia	617 kg·m²
Distance from CG to front axle	1.013 m
Distance from CG to rear axle	0.702 m
Track width	1.3 m
Suspension type	Rack and pinion type Steer-by-Wire (SBW)
Steering system	0.302 m
Tire radius	0.302 m
Driving system	
Driving type	Rear In-wheel motor drive
Maximum motor torque	340 Nm
Maximum power	10.7 kW
Maximum speed	1500 rpm

The specifications of the experimental electric vehicle are listed in Table 1.

3. DESIGN OF ROBUST YAW STABILITY CONTROLLER

The configuration of the proposed control system is shown in Figure 3. The overall control law of the proposed control system is described as follows:

- The desired yaw rate is obtained from the driver's steering command, δ_{cmd}, and the vehicle speed, v_x.
- The inner loop SA-DOB contributes to disturbance rejection by feeding a compensation steering angle into a control input to the steering motor. This compensation steering angle is the difference between a command steering angle to the vehicle and a filtered output from an inverse model of the nominal yaw model, $P_n^{-1}(s)$.
- The outer loop tracking controller, $C(s)$, is designed to compensate the steering angle for the measured yaw rate to track the desired yaw rate within the performance specifications.
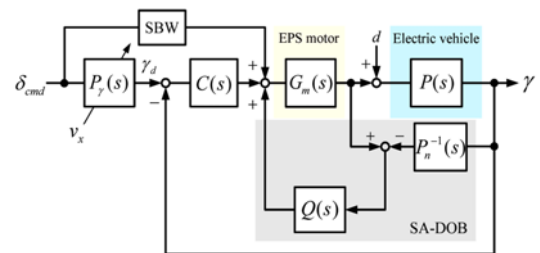

Figure 3. Block diagram of the proposed control system.

3.1. Desired Yaw Model and EPS Motor Control

The aim of the yaw stability control is to improve the vehicle steadiness and transient response properties, thus enhancing the vehicle handling performance and maintaining stability in cornering maneuvers (i.e., to make the vehicle follow the driver's cornering command). The desired vehicle responses are defined based on the driver's cornering intention (e.g., the driver's steering command and the vehicle speed). Usually, the vehicle responses during steady state cornering (i.e., $\dot{\gamma} = \dot{\beta} = 0$) are used as the desired vehicle responses. A desired yaw rate response for a given steering angle and vehicle velocity is obtained as follows:

$$\gamma_d(s) = \left(\frac{\omega_{yaw}^2}{s^2 + 2\zeta\omega_{yaw}s + \omega_{yaw}^2} \right) \cdot \frac{v_x}{(l_f + l_r)(1 + K_s v_x^2)} \cdot \delta_{cmd} \quad (9)$$

where ω_{yaw}, ζ are the cutoff frequency and the damping coefficient of a second-order yaw model filter, respectively, (in this paper, $\omega_{yaw} = 30 rad/s$, $\zeta = 0.8$); and K_s is the vehicle stability factor, which describes the steering characteristics of the vehicles and is defined by

$$K_s = \frac{m(l_r C_r - l_f C_f)}{2l^2 C_f C_r} \quad (10)$$

Here, the sign of $l_r C_r - l_f C_f$ represents vehicle motion behavior by steering action, and the steering characteristics are classified as follows:

$l_r C_r - l_f C_f > 0$: under steering
$l_r C_r - l_f C_f = 0$: neutral steering
$l_r C_r - l_f C_f < 0$: over steering

Figure 4 shows the configuration of the EPS motor control system. The EPS motor under position control is used to set the total front wheel steering angle. By considering linearized EPS motor dynamics, and thereby designing a feedback controller (i.e., P control), a closed-loop transfer function can be simplified as

$$G_m(s) = \frac{\delta_f(s)}{\delta_f^*(s)} \approx \frac{\omega_m}{s + \omega_m} \quad (11)$$

where ω_m is set to 30 rad/s.

To verify the control efficacy of the EPS motor controller, an experiment is conducted with an EPS motor control at a vehicle speed of 40 km/h. The results are shown in Figure 5. The reference steering angle, δ_f^*, is
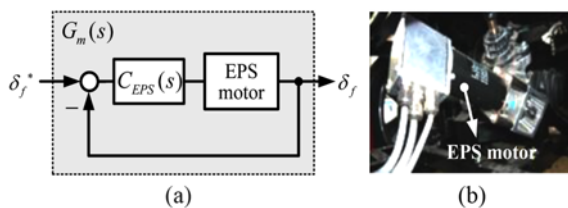
Figure 4. EPS motor control system: (a) a block diagram of the EPS motor controller and (b) an EPS motor.
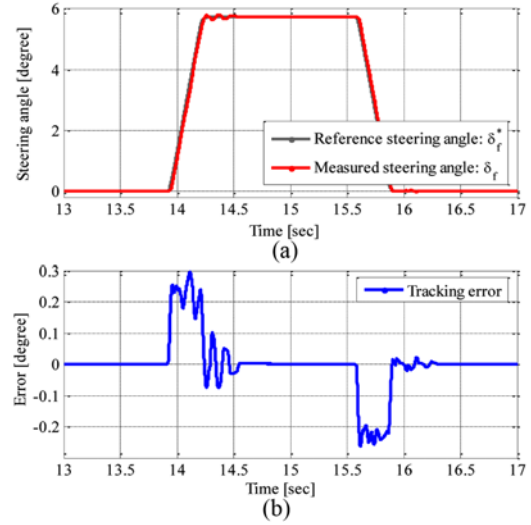
Figure 5. Experimental results of the EPS motor control: (a) steering angle and (b) tracking error.

generated by the driver's steering command and the measured steering angle, δ_f, is the sensor measurement of the EPS motor angle. As shown in Figure 5, the measured steering angle tracks the reference steering angle with a small tracking error.

3.2. Design of a Feedback Controller

The control objective is to design a robust yaw stability controller that enhances yaw tracking performance and disturbance rejection. The feedback control design problem is formulated as a two feedback loop design, which is composed of an inner SA-DOB loop design and an outer tracking control loop design.

In the outer tracking control loop design, the controller, $C(s)$, is designed based on the nominal yaw model so that the performance specifications can be satisfied. Hence, it is assumed that the inner SA-DOB loop behaves like a nominal yaw model. The tracking controller, $C(s)$, is designed to improve the desired yaw rate tracking performances. In this paper, is designed as a conventional PI controller.

$$C(s) = K_p \left(1 + \frac{1}{\tau_I s} \right) \quad (12)$$

where K_p and τ_I are the feedback gains, which are chosen based on robust performance and stability conditions.

In the inner SA-DOB loop design, it is important to select a proper Q-filter (i.e., $Q(s)$ in Figure 3). For design simplicity, the Q-filter is designed as a low-pass filter, which has the following design constraints:

$$\begin{cases} Q(0) = 1 \\ Q(s)P_n^{-1}(s) \in RH_\infty \end{cases} \quad (13)$$

In the proposed control system, the first-order low-pass filter with a unit DC gain is selected as the $Q(s)$ and is expressed as follows:
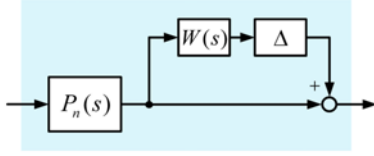
Figure 6. Multiplicative perturbation model.

$$Q(s) = \frac{\omega_{DOB}}{s + \omega_{DOB}} \tag{14}$$

where ω_{DOB} is a design parameter.

In the closed-loop feedback control system, as shown in Figure 3, the sensitivity function $S(s)$ and the complementary sensitivity function $T(s)$ are defined as follows:

$$S(s) = \frac{1 - G_m(s)Q(s)}{1 + P_n(s)G_m(s)C(s)} \tag{15}$$

$$T(s) = \frac{G_m(s)(P_n(s)C(s) + Q(s))}{1 + P_n(s)G_m(s)C(s)} \tag{16}$$

Note that the sensitivity function and the complementary sensitivity function depend on an inner-loop SA-DOB and an outer-loop tracking controller. The Q-filter and the feedback control gains are selected to satisfy the robust performance and robust stability conditions that are defined on the frequency domain.

To account for a wide variety of model uncertainties, including vehicle parameter variations, the multiplicative perturbation model, shown in Figure 4, is used. As shown in Figure 2, tire cornering stiffness is predominantly dependent on tire-road conditions. In this paper, the multiplicative perturbation model is used to consider model variations in terms of tire characteristics (e.g., $C_f \in$ (5000, 15000), which is obtained from field test data). The multiplicative perturbation model is given by

$$\tilde{P}(s) = P_n(s)[1 + W(s)\Delta(s)] \tag{17}$$

where $\tilde{P}(s)$ is the member of a set of vehicle models; is a nominal vehicle model; $\Delta(s)$ is the random stable function with bounded magnitude (i.e., $\|\Delta(s)\|_\infty < 1$); and $W(s)$, which is the stable boundary function of the multiplicative model uncertainty, accounts for the magnitude of the frequency-dependent uncertainty. To guarantee the robust stability of a closed-loop system with respect to multiplicative model uncertainty, the complementary sensitivity function, $W_2(s)$, is designed to satisfy the following conditions:

$$|W(s)\Delta s| \le |W_2(s)| \quad \text{AND} \quad |T(s)W_2(s)|_\infty < 1 \tag{18}$$

Similarly, to guarantee the robust performance, the robust performance condition is applied. Necessary and sufficient conditions for robust performance are given by

$$\|S(s)W_1(s)\| + \|T(s)W_2(s)\|_\infty \le 1, \ \forall \omega \in [0; +\infty] \tag{19}$$

where $W_1(s)$ and $W_2(s)$ are the sensitivity weighting

function and the complementary sensitivity weighting function, respectively. $W_2(s)$ is chosen to impose an upper bound on the control system bandwidth based on the multiplicative model uncertainty bound. Similarly, $W_1(s)$ is chosen to impose the lower bound of the control system bandwidth based on nominal performances (e.g., steady state error: $s.s.e < 5\%$; and disturbance rejection at a frequency region of interest: 10 rad/s). These two weighting functions are selected as follows:

$$W_1(s)\frac{s + 10.3}{3(s + 10 \cdot 0.05)}, \quad W_2(s)\frac{s + 20 \cdot 0.5}{3(s + 20 \cdot 2)} \tag{20}$$

Figures 7 and 8 show the frequency characteristics of a closed-loop system. Because the magnitude of a sensitivity function is less than that of the inverse function of model uncertainty, the robust stability condition for the model uncertainty is satisfied. The proposed control system contributes to the improvement of the sensitivity characteristics at low frequency, as shown in Figure 7.

4. SIMULATION AND EXPERIMENT

4.1. Simulation
The control performance of the proposed control system
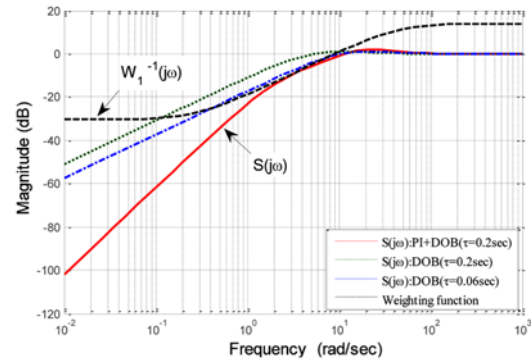
Figure 7. Frequency characteristics of the closed-loop system ($v_x = 40$ km/h): Bode plot of a sensitivity function.
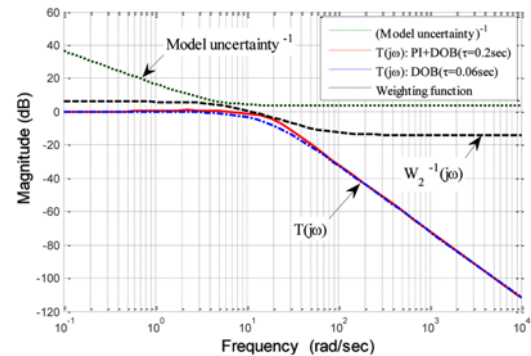
Figure 8. Frequency characteristics of the closed-loop system ($v_x = 40$ km/h): Bode plot of a complementary sensitivity function.
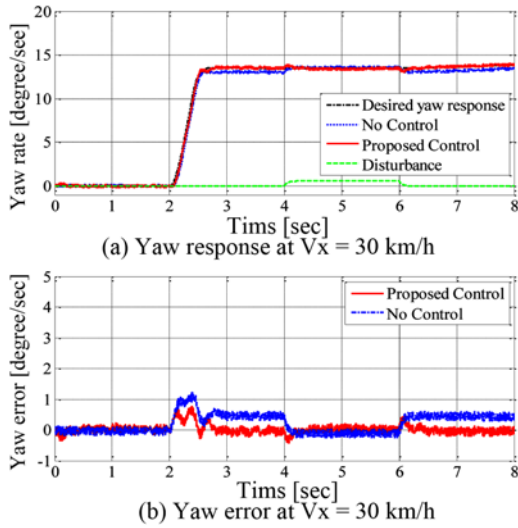
Figure 9. Simulation results: control in the under-steering case.
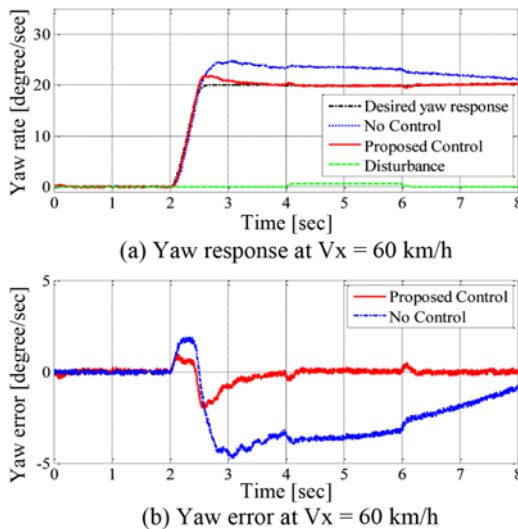

Figure 10. Simulation results: control in the over-steering case.

was verified through computer simulations using CarSim. A control algorithm was implemented on a CarSim model corresponding to actual electric vehicles, as shown in Figure 11. A step steering test with a steering wheel angle of 45 degrees was performed to verify the disturbance rejection and tracking performances. The yaw disturbance is intentionally inserted at $t = 4$sec. The simulation results for vehicles with $v_x = 30$ km/h show good tracking and disturbance rejection performances, as shown in Figures 9 (a) and 9 (b), respectively. Similar simulation results were shown in Figure 10 for $v_x = 60$ km/h.

To verify the effectiveness and robustness of the proposed control system, simulations on a slippery road,
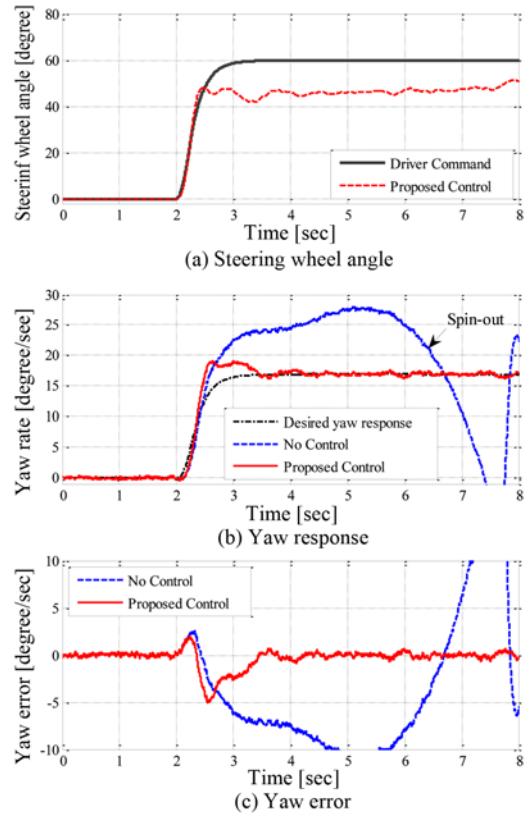

Figure 11. Simulation results of a step steer test at $v_x = 60$ km/h on a slippery road.

e.g., $\mu \approx 0.4$, were performed and the results are shown in Figure 11. A step steering command is applied, and the controlled steering angles are represented in Figure 11 (a). Figures 11 (b) and 11 (c) show the results of the yaw rate control and the calculated yaw error, respectively. In a no-control case, the vehicle undergoes a spin-out phenomenon, indicating a loss of stability, as shown in Figure 11 (b) (see the dotted blue line). Conversely, in the control case, the vehicle response is well matched with the desired yaw response without a noticeable error. Although there is a small error due to the relatively conservative control design during transient steering, the vehicle yaw stability is completely satisfied. From these results, we can confirm that the proposed yaw stability control system is robust against the vehicle speed and road conditions.

4.2. Experiment
The proposed controller was implemented in the experimental in-wheel-motor-driven electric vehicle, which was developed by the authors' research team, as shown in Figure 12 (for further information, see Nam et al., 2012). The experimental electric vehicle used in this research has the following special features:

• In-wheel motors are mounted in each wheel, and we can completely and independently control each wheel torque

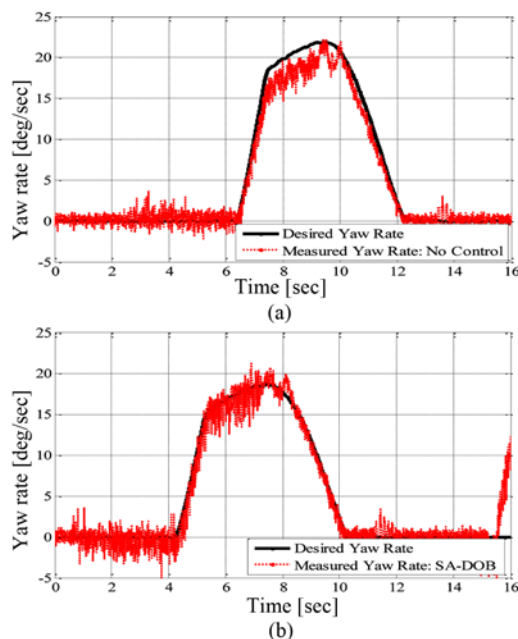Figure 12. In-wheel-motor-driven electric vehicle.

Figure 13. Experimental results: (a) without control and (b) with the proposed control.

for vehicle motion control.
- Active front steering control is realizable through a SbW system with an EPS motor as shown in Figure 4.

Figure 13 shows the experimental results of the proposed yaw stability control realized by active front steering control. Although the experiments at constant vehicle speed were not carried out due to limited driving conditions (e.g., limited driving space), the effectiveness of the proposed control system can be confirmed by comparing Figure 13 (a) with Figure 13 (b).

In the case of Figure 13 (a), which is the result of an experiment without control, the yaw error is evident (i.e., yaw error=desired yaw rate-measured yaw rate). Conversely, the experimental result for the vehicle with the proposed control shows relatively good tracking performance. The vehicle yaw response with the proposed control tracks well with the desired yaw rate trajectory.

5. CONCLUSION

In this paper, a robust yaw stability control system for in-wheel-motor-driven electric vehicles with an SbW system is proposed and evaluated. In contrast to conventional yaw stability control systems for electric vehicles, which are based on independent torque control of in-wheel driving motors, the proposed yaw stability control system is realized by active front steering control through an SbW system. The control system is composed of an inner loop SA-DOB to reject disturbances and an outer loop tracking controller to achieve nominal control performances. The controller, $C(s)$, and the Q-filter are designed based on robust control design methods to account for model variations in the nominal vehicle yaw model. An advantage of the proposed yaw stability controller is that it is possible to track the desired vehicle responses without information about road conditions and frequent torque control of driving motors, which decreases acceleration performance during cornering and the driver's comfort level. The practical application of an SbW system to a vehicle control system for electric vehicles is validated through experiments. Simulation and experimental results show that the proposed yaw stability controller enhances vehicle yaw stability within linear tire regions.

REFERENCES

Ackermann, J. and Bünte, T. (1997). Automatic car steering control bridges over the driver reaction time. *Kybernetika* **33**, **1**, 61−74.

Canale, M., Fagiano, L., Ferrara, A. and Vecchio, C. (2009). Comparing internal model control and sliding-mode approaches for vehicle yaw control. *IEEE Trans. Intell. Transp. Syst.* **10**, **1**, 31−41.

Chan, C. C. (2002). The state of the art of electric and hybrid vehicles. *Proc. IEEE* **90**, **2**, 247−275.

Doyle, J. C., Francis, B. A. and Tannenbauml, A. R. (1992). *Feedback Control Theory*. Macmillan Publishing Company. New York.

Falcone, P., Borrelli, F., Asgari, J., Tseng, H. E. and Hrovat, D. (2007). Predictive active steering control for autonomous vehicle systems. *IEEE Trans. Control Syst. Technol.* **15**, **3**, 566−580.

Fujimoto, H., Saito, T. and Noguchi, T. (2004). Motion stabilization control of electric vehicle under snowy conditions based on yaw-moment observer. *Proc. IEEE AMC*, 35−40.

Fujimoto, H., Tsumasaka, A. and Noguchi, T. (2005). Direct yaw-moment control of electric vehicle based on cornering stiffness estimation. *Proc. IEEE IECON*,

2626–2631.

Gvenc, B. A., Bnte, T., Odenthal, D. and Gven, L. (2004). Robust two degree-of-freedom vehicle steering controller design. *IEEE Trans. Control Syst. Technol.* **12**, **4**, 627–636.

Gvenc, B. A., Gven, L. and Regruto, S. (2009). Robust yaw stability controller design and hardware-in-the-loop testing for a road vehicle. *IEEE Trans. Veh. Technol.* **58**, **2**, 555–571.

Hori, Y. (2004). Future vehicle driven by electricity and control-research on four-wheel-motored "UOT Electric March II". *IEEE Trans. Ind. Electron.* **51**, **5**, 654–962.

Nam, K., Fujimoto, H. and Hori, Y. (2012). Lateral stability control of in-wheel-motor-driven electric vehicles based on sideslip angle estimation using lateral tire force sensors. *IEEE Trans. Veh. Technol.* **61**, **5**, 1972–1985.

Nam, K., Oh, S., Fujimoto, H. and Hori, Y. (2010). Robust yaw stability control for electric vehicles based on steering angle-disturbance observer (SA-DOB) and tracking control design. *Proc. IEEE IECON*, 1943–1948.

Ohara, H. and Murakami, T. (2008). A stability control by active angle control of front-wheel in a vehicle system. *IEEE Trans. Ind. Electron.* **55**, **3**, 1277–1285.

Sakai, S., Sado, H. and Hori, Y. (1999). Motion control in an electric vehicle with four independently driven in-wheel motors. *IEEE/ASME Trans. Mechatron.* **4**, **1**, 9–16.

Umeno, T. and Hori, Y. (1991). Robust speed control of DC servomotors using modern two degrees-of-freedom controller design. *IEEE Trans. Ind. Electron.* **38**, **5**, 363–368.